RUTGERS

Anti-Windup and Control Barrier Functions

“EuroGNC Control Barrier Functions in Aerospace" Workshop

May 4, 2026

Laurent Burlion

Outline

Background

- Motivation
- Output to Input Saturation Transformation (OIST)
- Links between Output to Input Saturation Transformation (OIST) & CBFs

A few technical results

- OIST and bounds overlapping
- Anti-windup designs
- OIST robustness using interval methods (OISTer)

Aerospace applications

Collaborators

Students:

- Emmanuel Chambon, "*Frequency and Time-domain Constrained Control of linear systems. Application to a flexible launch vehicle*", *Ph.D dissertation,* 2016.
- Corentin Chauffaut, postdoctoral researcher, 2015-2016
- Chengwei Zhao, Mike Fogel, Patanjali Maithani, Ph.D students, in progress.

Researchers:

- Henry de Plinval, Jean-Marc Biannic, Charles Poussot-Vassal, Pierre Apkarian (ONERA)
- Luca Zaccarian, Sophie Tarbouriech (LAAS)

I - Background

ENGINEERING

Background

- Motivation
- Output to Input Saturation Transformation (OIST)
- Links between Output to Input Saturation Transformation (OIST) & CBFs

A few technical results

- OIST and bounds overlapping
- Anti-windup designs
- OIST robustness using interval methods (OISTer)

Aerospace applications

Motivation

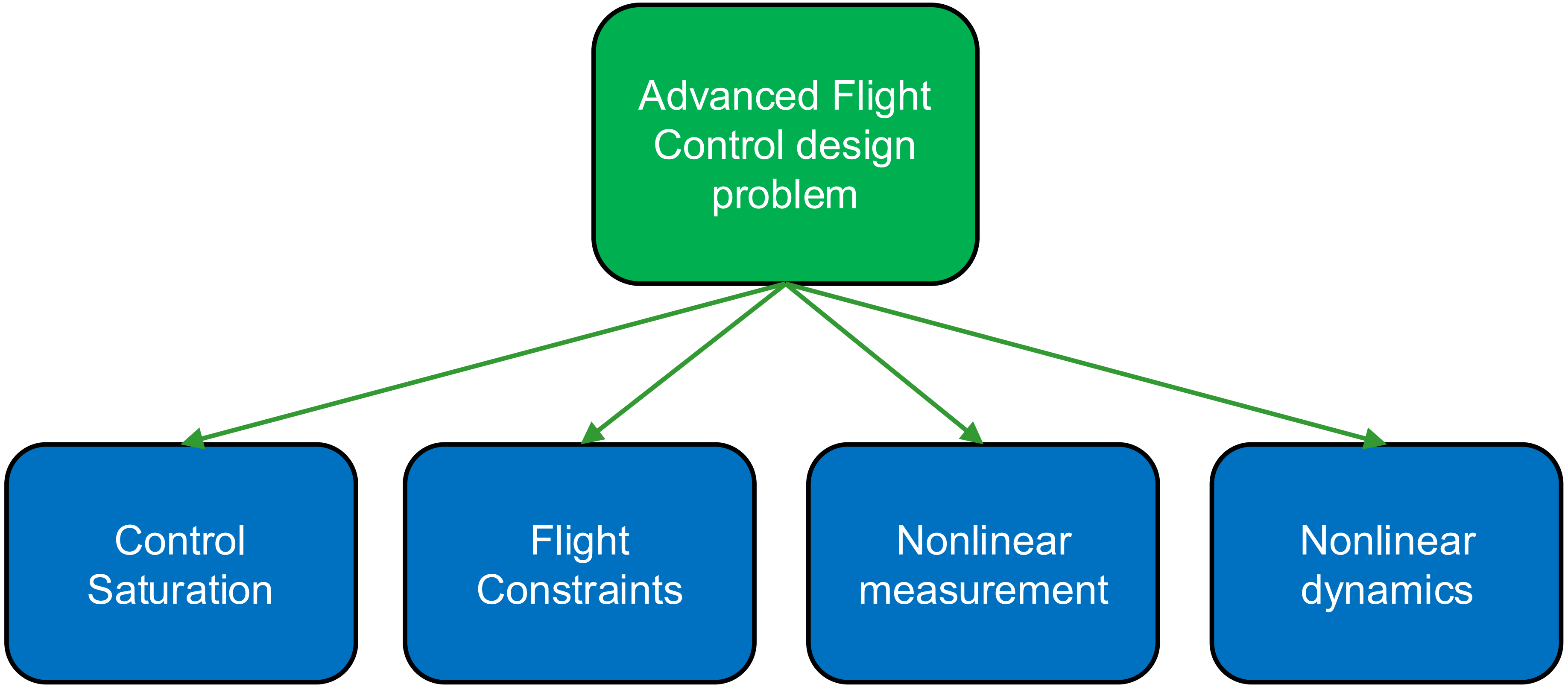
Advanced Flight Control design problem
Control Saturation
Flight Constraints
Nonlinear measurement
Nonlinear dynamics

Examples of flight constraints

ENGINEERING

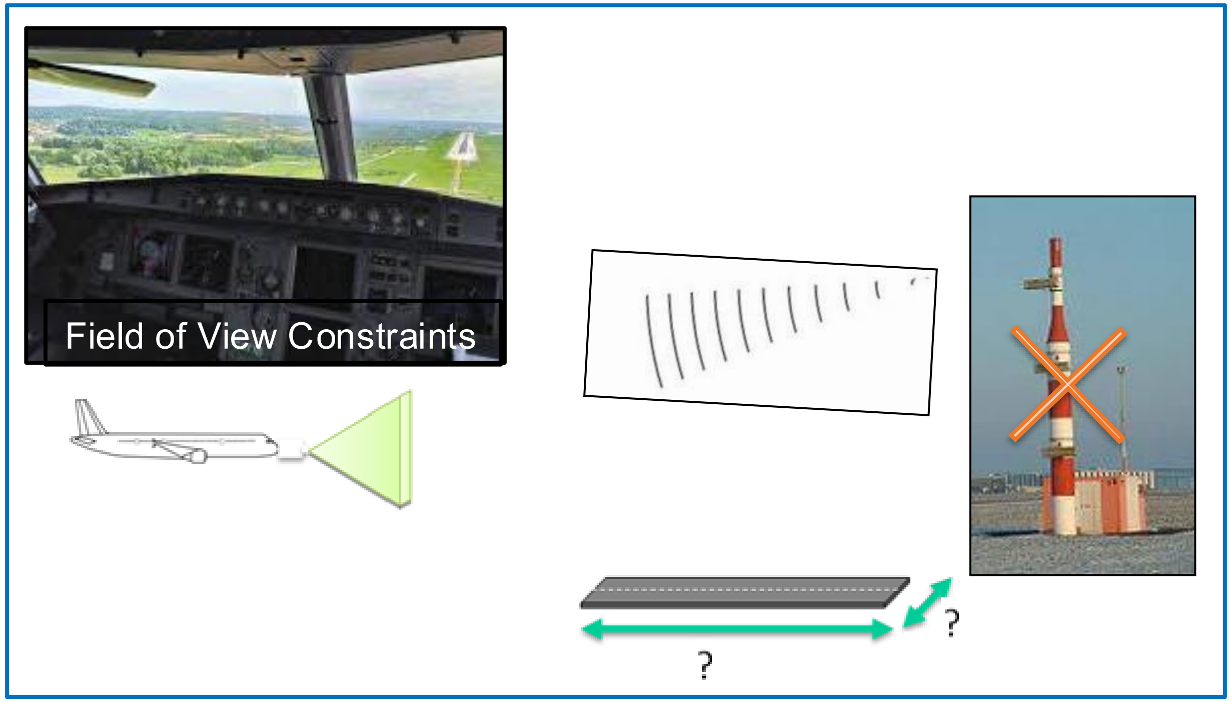

Model reference anti-windup

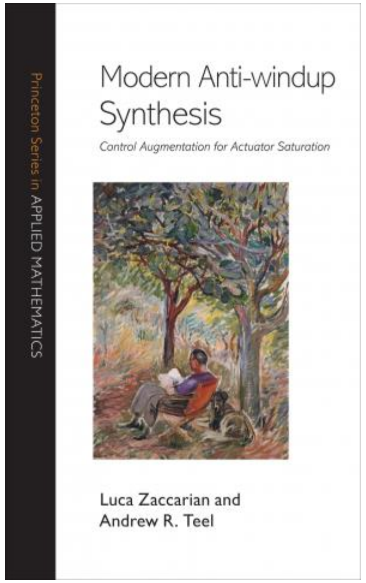

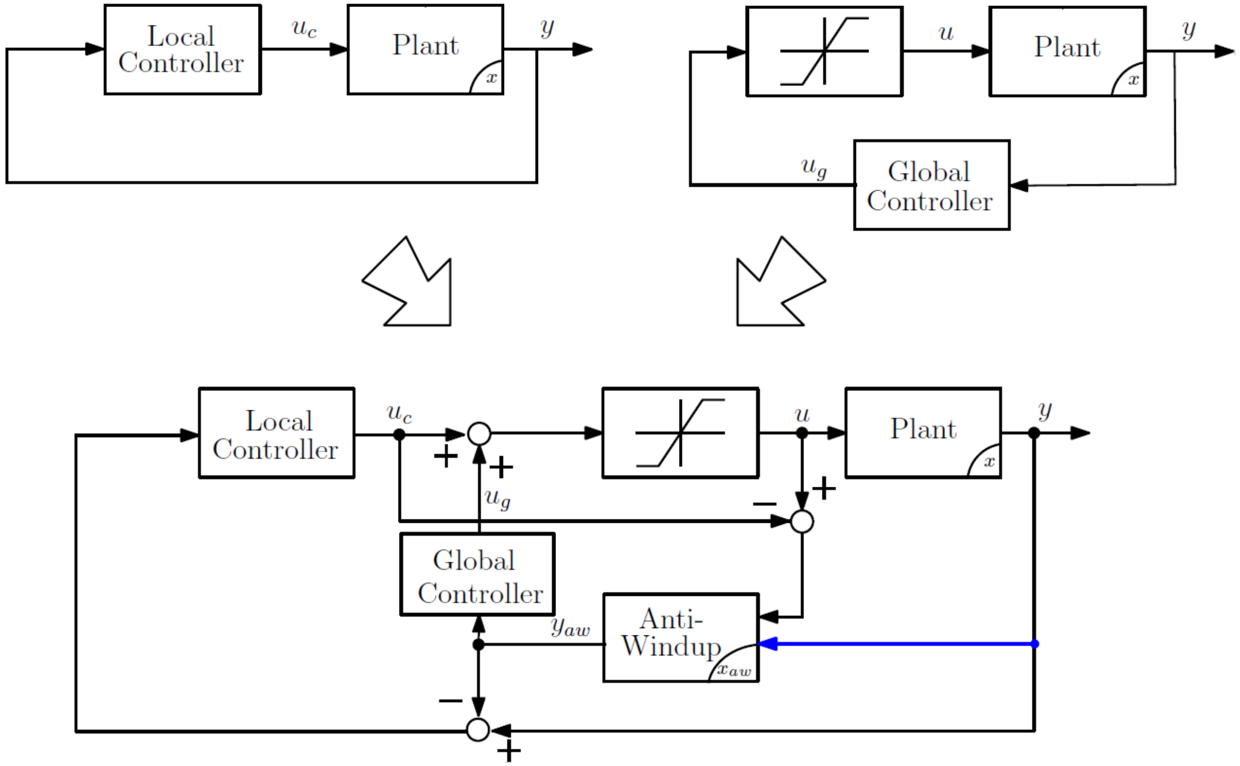

Output to Input Saturation Transformation

ENGINEERING

In many control applications, a common problem is to enforce bounds on specific outputs. In aerospace applications, this is required to design protection laws to keep the angle-of-attack in a safe region.

Problem formulation

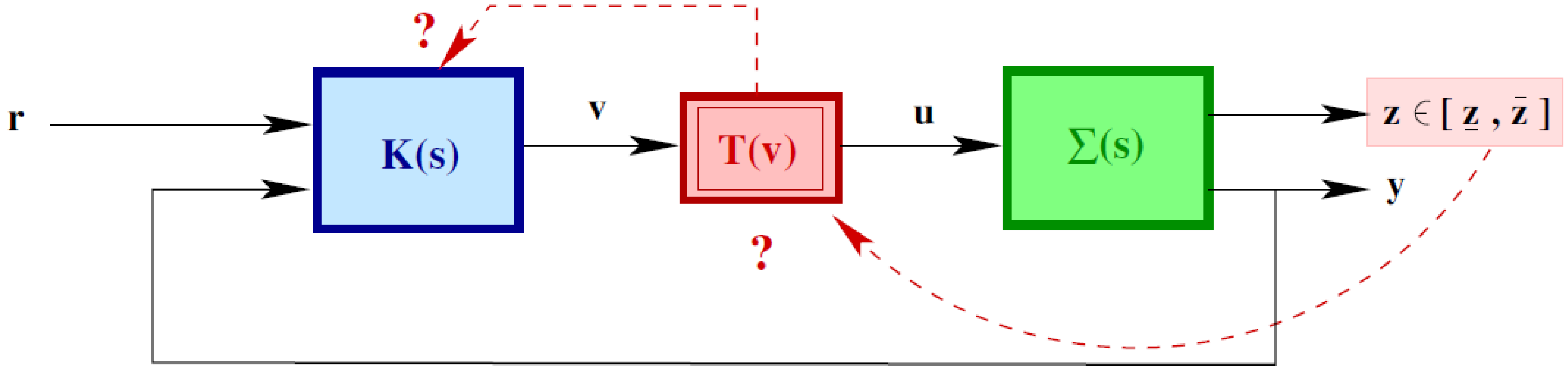

→ *Determine an "anti-windup compatible"* **input transformation** $u = T(v)$ *such that a given output* $z = Cx + Du \in [\underline{z}\,,\ \overline{z}]$.

Output to Input Saturation Transformation

Case 1 : $D \neq 0 \;\rightarrow\; z = Cx + Du$

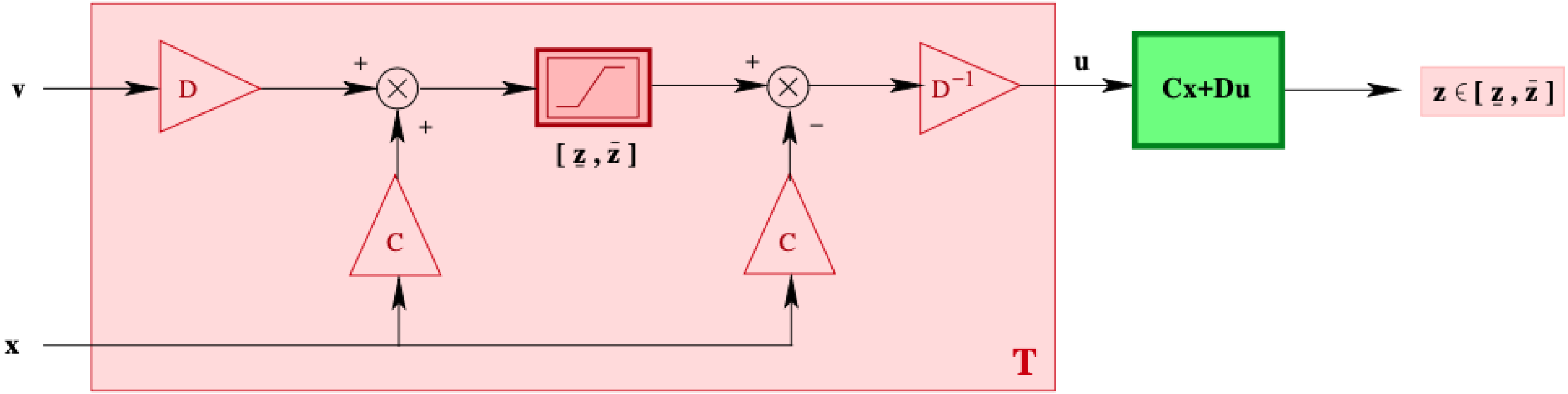

$$u = D^{-1}\left(\text{sat}(Cx + Dv) - Cx\right) \;\Rightarrow\; z = \text{sat}(Cx + Dv) \in [\underline{z}\,,\; \overline{z}]$$

Moreover :

$$Cx + Dv \in [\underline{z}\,,\; \overline{z}] \;\Rightarrow\; u = v$$

(From J-M. Biannic et al., 2017)

Output to Input Saturation Transformation

Case 2 : $D = 0 \;\rightarrow\; z = Cx\,,\; \dot{z} = CAx + CBu$ (with $CB \neq 0$)

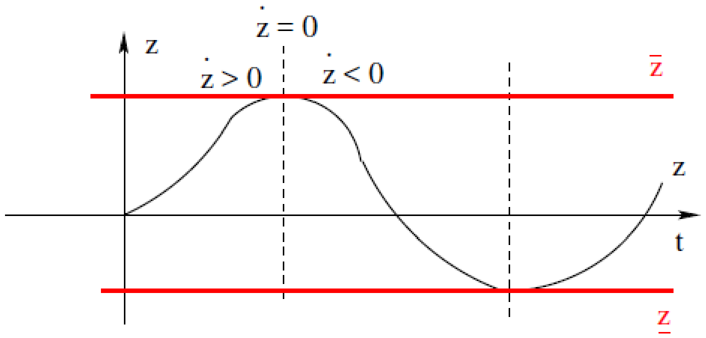

$$\tau \geq 0\,,\; \underline{z} - z \leq \tau \dot{z} \leq \overline{z} - z \quad \textbf{(1)}$$

$$\Downarrow$$

$$z \in [\underline{z}\,,\; \overline{z}]$$

From (1), it readily follows that :

$$\tau \dot{z} + z = C(I + \tau A)x + \tau CBu \in [\underline{z}\,,\; \overline{z}] \Rightarrow z \in [\underline{z}\,,\; \overline{z}]$$

$\Rightarrow$ back to **Case 1** with : $C \leftarrow C(I + \tau A)$ and $D \leftarrow \tau CB$

Remark : if $CB = 0$ ...

... *the above procedure can be applied recursively until* $CA^r B \neq 0$.

(From J-M. Biannic et al., 2017)

Nonlinear case

From Burlion,
Med 2012

$x \in \mathbb{R}^n; y \in \mathbb{R}$

$\dot{x} = f(x) + g(x)u \; ; \; y = h(x)$

Relative degree 1

$$y_{\min} \leq y(0) \leq y_{\max}$$
$$-\alpha(y - y_{\min}) \leq L_f h(x) + L_g h(x) u \leq -\alpha(y - y_{\max})$$

$\Rightarrow$

$$y_{\min} \leq y \leq y_{\max}$$

Relative degree r (by recursion)

Example 1 – Load alleviation of a combat aircraft

From Burlion,
Med 2012

The longitudinal dynamics of the combat aircraft is written

$$\begin{cases} \dot{\alpha} & = & q + k(Mach)N_z(Mach,\alpha)\cos(\alpha) \\ \dot{q} & = & W(Mach,\alpha,q) + B(Mach,\alpha,q)u \end{cases}$$

When the full state is available, our design leads to

$$u \in [h_1, h_2]$$

where :

$$\begin{cases} h_1 & = & \dfrac{K_{1,2}(N_{min}-N_z)-K_2\dot{N}_z-\frac{\partial N_z}{\partial\alpha}W-\frac{\partial^2 N_z}{\partial\alpha^2}\dot{\alpha}^2}{\frac{\partial N_z}{\partial\alpha}B} \\ h_2 & = & \dfrac{K_{1,2}(N_{max}-N_z)-K_2\dot{N}_z-\frac{\partial N_z}{\partial\alpha}W-\frac{\partial^2 N_z}{\partial\alpha^2}\dot{\alpha}^2}{\frac{\partial N_z}{\partial\alpha}B} \end{cases}$$

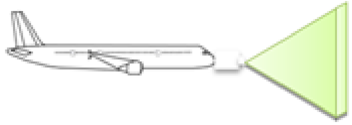

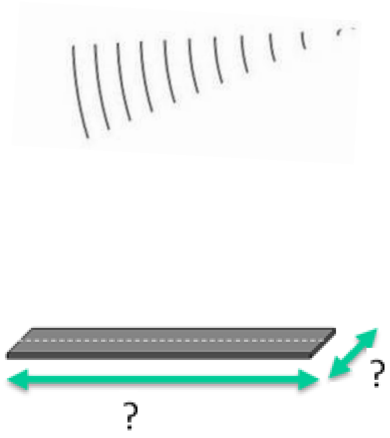

Nonlinear measurement

$$\begin{cases} y_1 = \dfrac{\Delta_z}{x} \\ y_2 = \dfrac{\Delta_y}{x} \end{cases}$$

From Burlion et al.,
ICRA 2013

$$w_1 := \frac{v_2}{v_1} \quad \& \quad w_2 := \frac{v_3}{v_1}$$

- Field of view constraints

$$\begin{pmatrix} p^{sat} \\ q^{sat} \end{pmatrix} = [M_z(x)]^{-1} \begin{pmatrix} Sat_{h_1^1(x)}^{h_2^1(x)}\left(\frac{v_3^* p + v_3^* w_1 q}{v_1}\right) \\ Sat_{h_1^2(x)}^{h_2^2(x)}\left(\frac{-v_2^* p + (v_1^* + v_3^* w_2) q}{v_1}\right) \end{pmatrix}$$

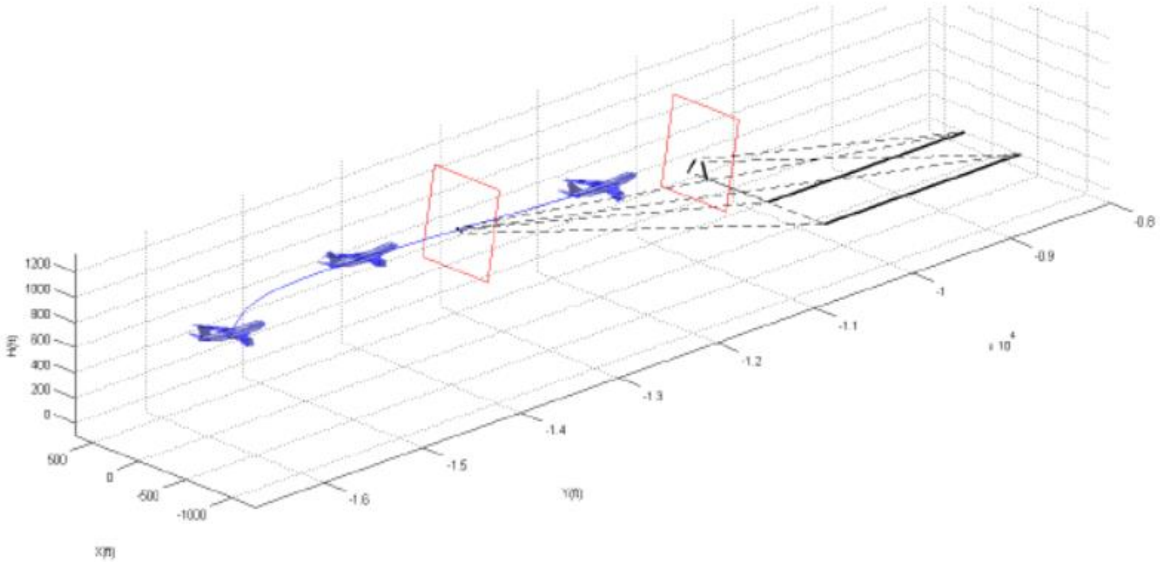

Example 2- Vision based automatic landing

From Burlion et al., ICRA 2013

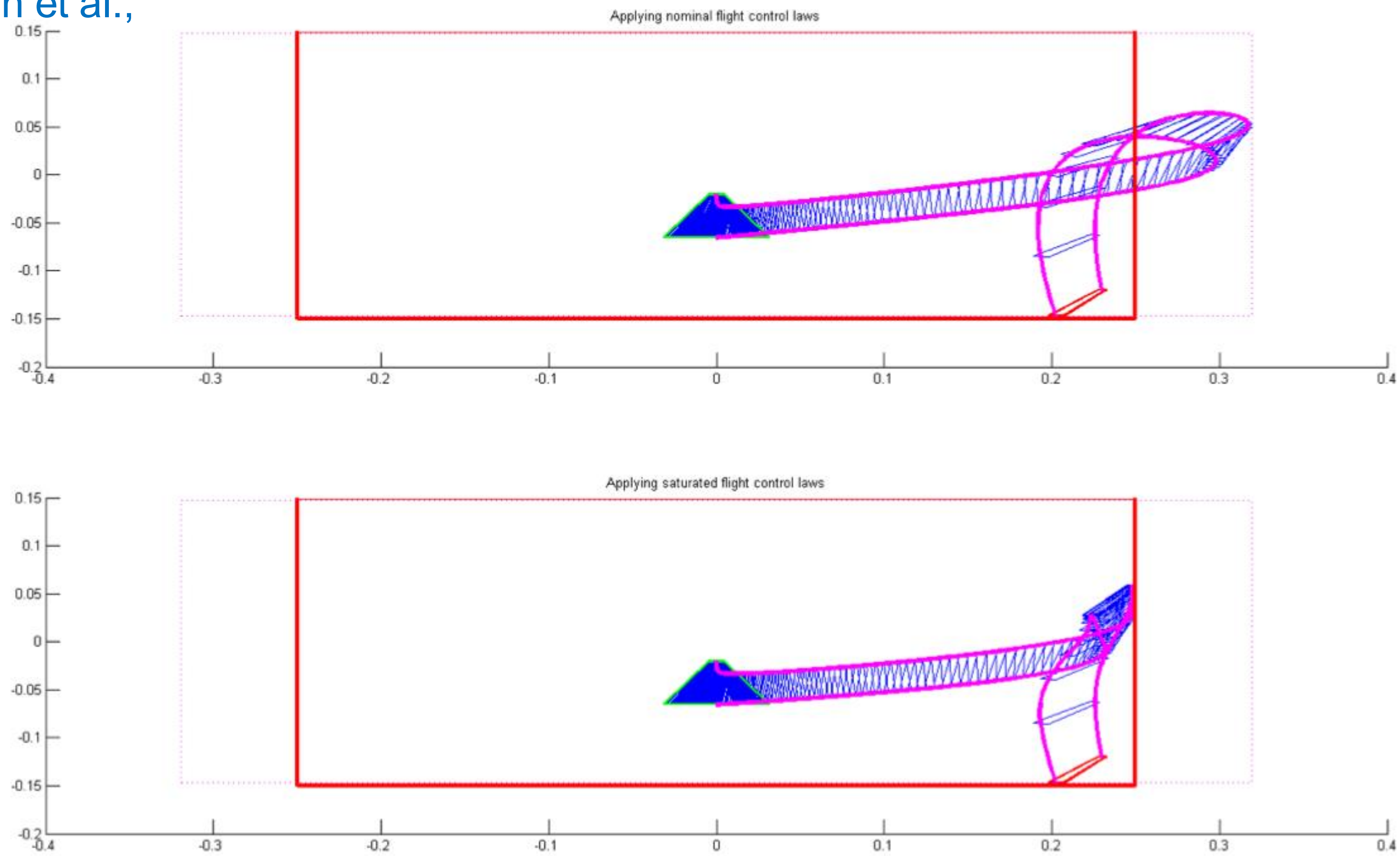

Burlion Research Group

Links between OIST and CBFs

$x \in \mathbb{R}^n; y \in \mathbb{R}$

$$\dot{x} = f(x) + g(x)u \; ; \; y = h(x)$$

<u>Key observation:</u>

CBF framework:

$$C = \{x : b(x) \geq 0\}$$

$b(.)$ is a CBF if $\exists$ a class $\mathcal{K}$ function α s.t

$$sup_{u \in U} L_f b(x) + L_g b(x)u + \alpha(b(x)) \geq 0, \forall x \in C$$

OIST framework: $\mathcal{C} = \mathcal{C}_{\min} \cap \mathcal{C}_{\max} := \{x : h(x) + y_{\min} \geq 0\} \cap \{x : -h(x) + y_{\max} \geq 0\}$

$y_{\min}$ $x(0) \in C$ $y_{\max}$

$$L_f(-h(x)) + L_g(-h(x))u + \alpha(-(h(x) + y_{\max})) \geq 0$$

$$L_f h(x) + L_g h(x)u + \alpha(h(x) - y_{\min}) \geq 0$$

$\Rightarrow$ $x(t) \in \mathcal{C}, t \geq 0$

Burlion Research Group

Links between OIST and CBFs

$x \in \mathbb{R}^n; y \in \mathbb{R}$

$$\dot{x} = f(x) + g(x)u \; ; \; y = h(x)$$

Conclusion:

$$\begin{aligned} OIST(u^c) = \quad & \min_u \quad (u^c - u)^2 \\ & s.t \\ & L_f(-h(x)) \quad +L_g(-h(x))u + \alpha(-(h(x) + y_{\max})) \geq 0 \\ & L_f h(x) \quad +L_g h(x)u + \alpha(h(x) - y_{\min}) \geq 0 \end{aligned}$$

Note that this observation generalizes to higher degrees (HOCBFs)
See (Burlion 2012) for a higher degree version of OIST.

II – A few technical results

Background
- Motivation
- Output to Input Saturation Transformation (OIST)
- Links between Output to Input Saturation Transformation (OIST) & CBFs

A few technical results
- OIST and bounds overlapping
- Anti-windup designs
- OIST robustness using interval methods (OISTer)

Aerospace applications of OISTer

Saturation bounds overlap

Simple Example

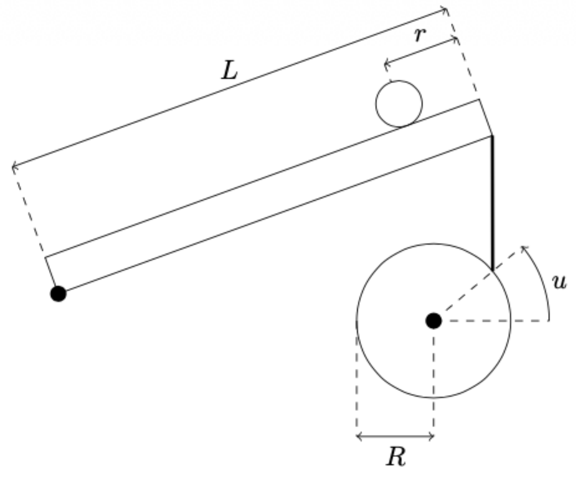

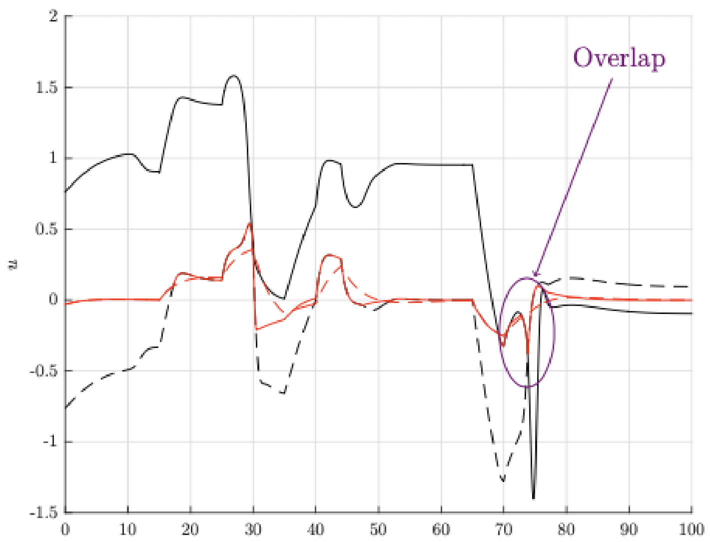

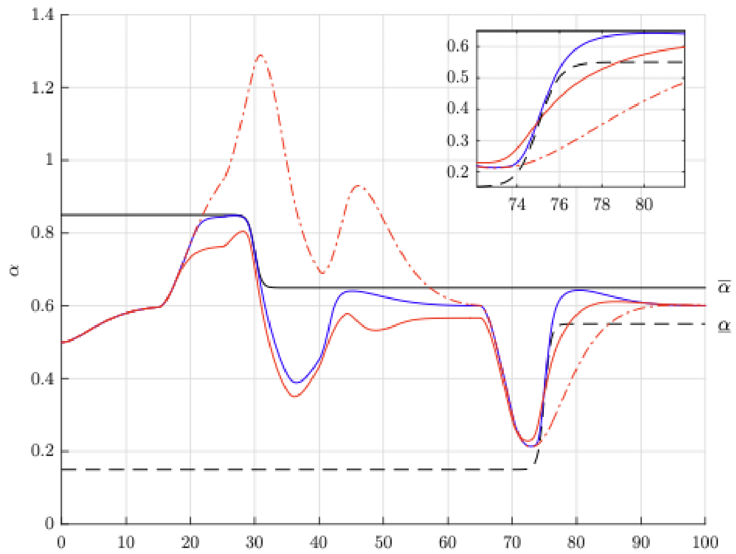

Saturation bounds overlap

Following [Chambon et al, 2016]

$$(\mathbf{G})\begin{cases}\dot{\boldsymbol{x}} = \mathbf{A}\boldsymbol{x} + \mathbf{B_u}u + \mathbf{B_d}\boldsymbol{d}\\ \boldsymbol{y} = \boldsymbol{x} + \mathbf{D_d}\boldsymbol{d}\end{cases}$$

$$(\mathbf{K})\begin{cases}\dot{\boldsymbol{x}}_K = \mathbf{A_K}\boldsymbol{x}_K + \mathbf{B_K}\boldsymbol{u}_K\\ y_K = \mathbf{C_K}\boldsymbol{x}_K + \mathbf{D_K}\boldsymbol{u}_K\end{cases}$$

$$\begin{aligned}\alpha &= \mathbf{C}_\alpha \boldsymbol{y}\\ &= \mathbf{C}_\alpha \boldsymbol{x} + \mathbf{C}_\alpha \mathbf{D_d}\boldsymbol{d}\\ &= \mathbf{C}_\alpha \boldsymbol{x} + \mathbf{D}_\alpha \boldsymbol{d}\end{aligned}$$

$$\begin{aligned}\underline{u}(t) = \frac{1}{\mathbf{C}_\alpha \mathbf{A}^{k-1}\mathbf{B_u}}\Big[&\underline{\alpha}_k(t) - \mathbf{C}_\alpha \mathbf{A}^k \boldsymbol{x}(t) + \textstyle\sum_{i=1,l_i=0}^{q} |\mathbf{D}_{\alpha i}| \max\left(\left|\underline{\boldsymbol{d}_i}^{(k)}(t)\right|, \left|\overline{\boldsymbol{d}_i}^{(k)}(t)\right|\right)\\ &+ \textstyle\sum_{i=1,l_i\neq 0}^{q} \sum_{j=l_i}^{k} \left|\mathbf{C}_\alpha \mathbf{A}^{j-1}\mathbf{B_d}\right| \max\left(\left|\underline{\boldsymbol{d}_i}^{(k-j)}(t)\right|, \left|\overline{\boldsymbol{d}_i}^{(k-j)}(t)\right|\right)\Big]\end{aligned}$$

$$\begin{aligned}\overline{u}(t) = \frac{1}{\mathbf{C}_\alpha \mathbf{A}^{k-1}\mathbf{B_u}}\Big[&\overline{\alpha}_k(t) - \mathbf{C}_\alpha \mathbf{A}^k \boldsymbol{x}(t) - \textstyle\sum_{i=1,l_i=0}^{q} |\mathbf{D}_{\alpha i}| \max\left(\left|\underline{\boldsymbol{d}_i}^{(k)}(t)\right|, \left|\overline{\boldsymbol{d}_i}^{(k)}(t)\right|\right)\\ &- \textstyle\sum_{i=1,l_i\neq 0}^{q} \sum_{j=l_i}^{k} \left|\mathbf{C}_\alpha \mathbf{A}^{j-1}\mathbf{B_d}\right| \max\left(\left|\underline{\boldsymbol{d}_i}^{(k-j)}(t)\right|, \left|\overline{\boldsymbol{d}_i}^{(k-j)}(t)\right|\right)\Big],\end{aligned}$$

Saturation bounds overlap

Proposed Solution:

(From Chambon et al. 2018)

1. Increase coefficients defining OIST (Rule of Thumb)
2. Design time-varying coefficients (Our contribution)

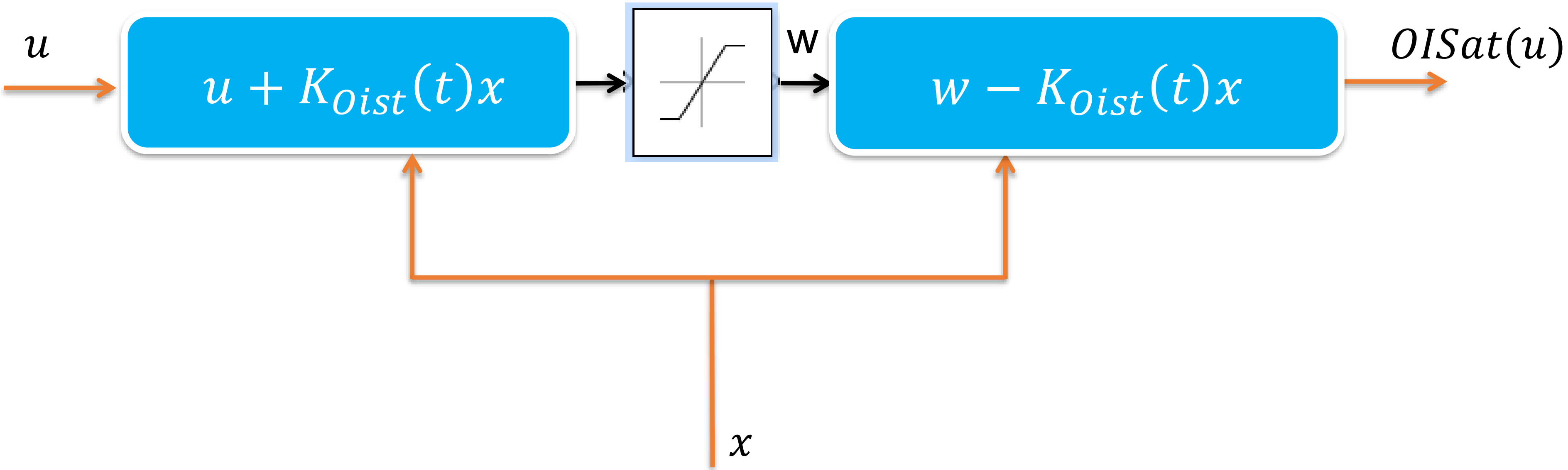

(From Chambon et al. 2018)

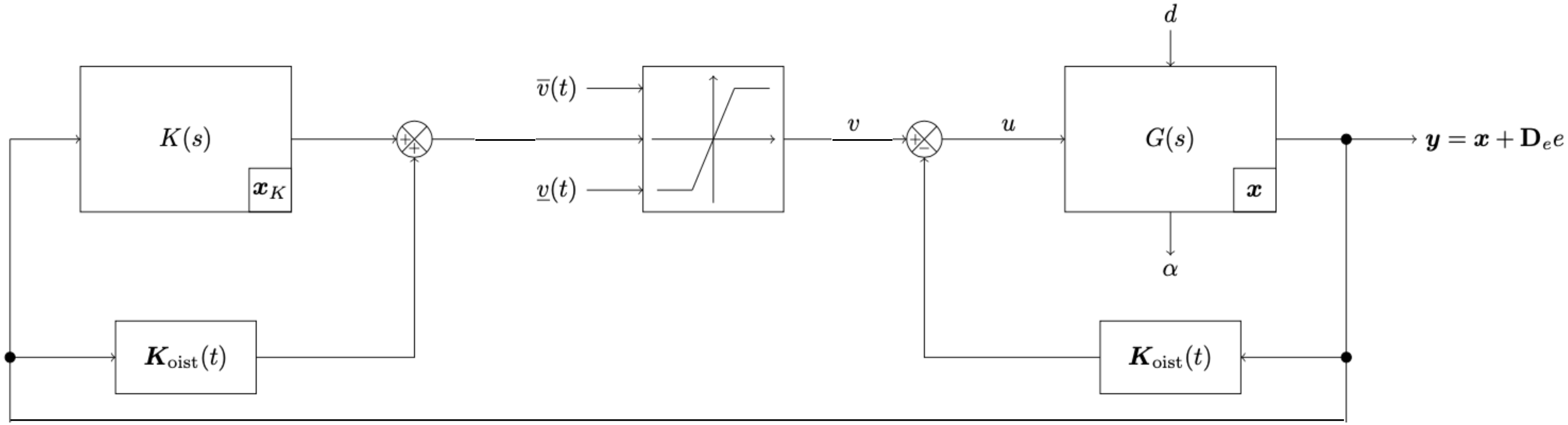

Stability and anti-windup design

(From Chambon et al. 2018)

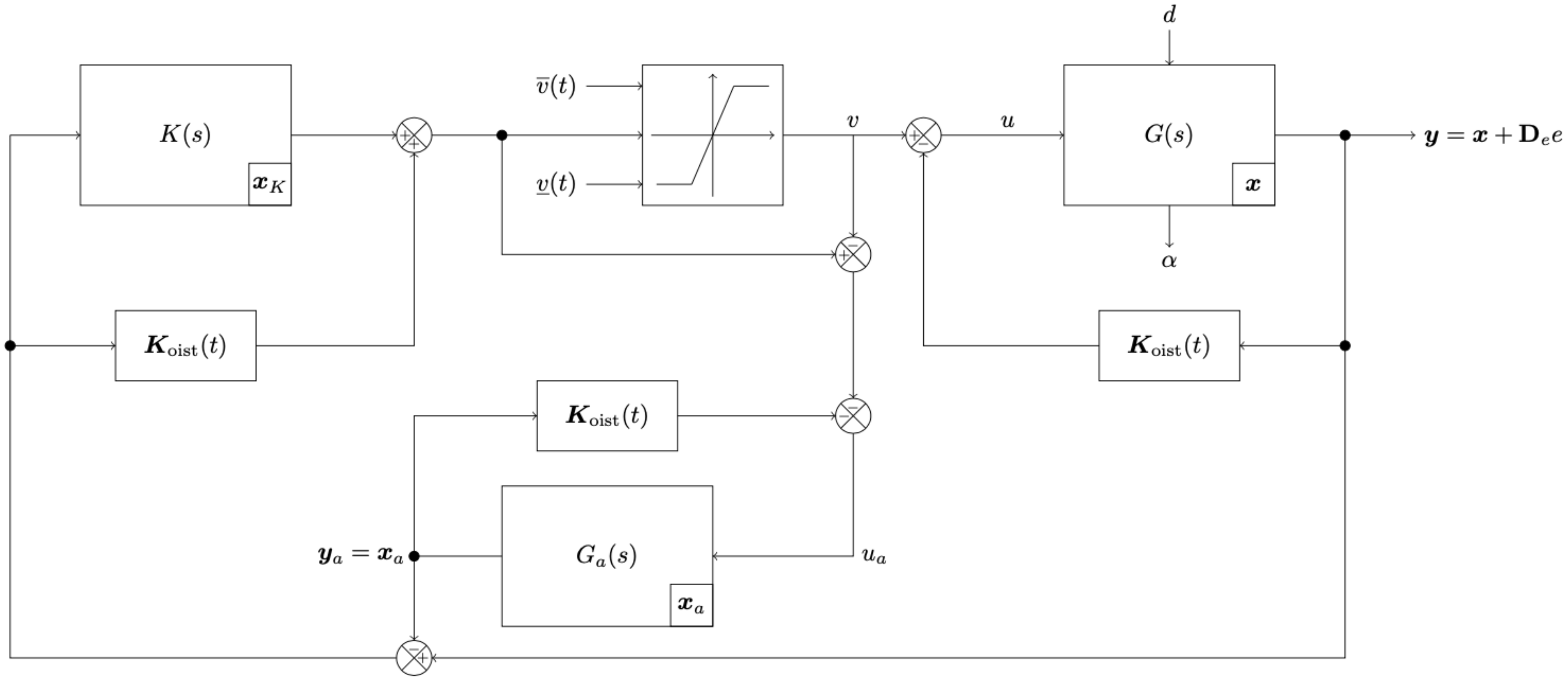

Guaranteed closed-loop stability for a minimum phase constrained output

Proved using AW structure as in [Herrmann et al, 2010)

Burlion Research Group

Stability and anti-windup design

Consider the Combat Aircraft example (Freire & Nicotra)

F-16 Pitch Dynamics

$$x = \begin{bmatrix}\theta & \dot{\theta} & \alpha_w & \delta_e & \delta_f\end{bmatrix}$$

$$u = \begin{bmatrix}\delta_{e,c} & \delta_{f,c}\end{bmatrix}$$

<u>Analysis</u>

- Dimension 7 after we applied a LQ-I controller
- Constrained output: the angle of attack
- Relative degree: 2
- 1 constraint & 2 control inputs: we only used the second input

Stability and anti-windup design

Combat Aircraft example

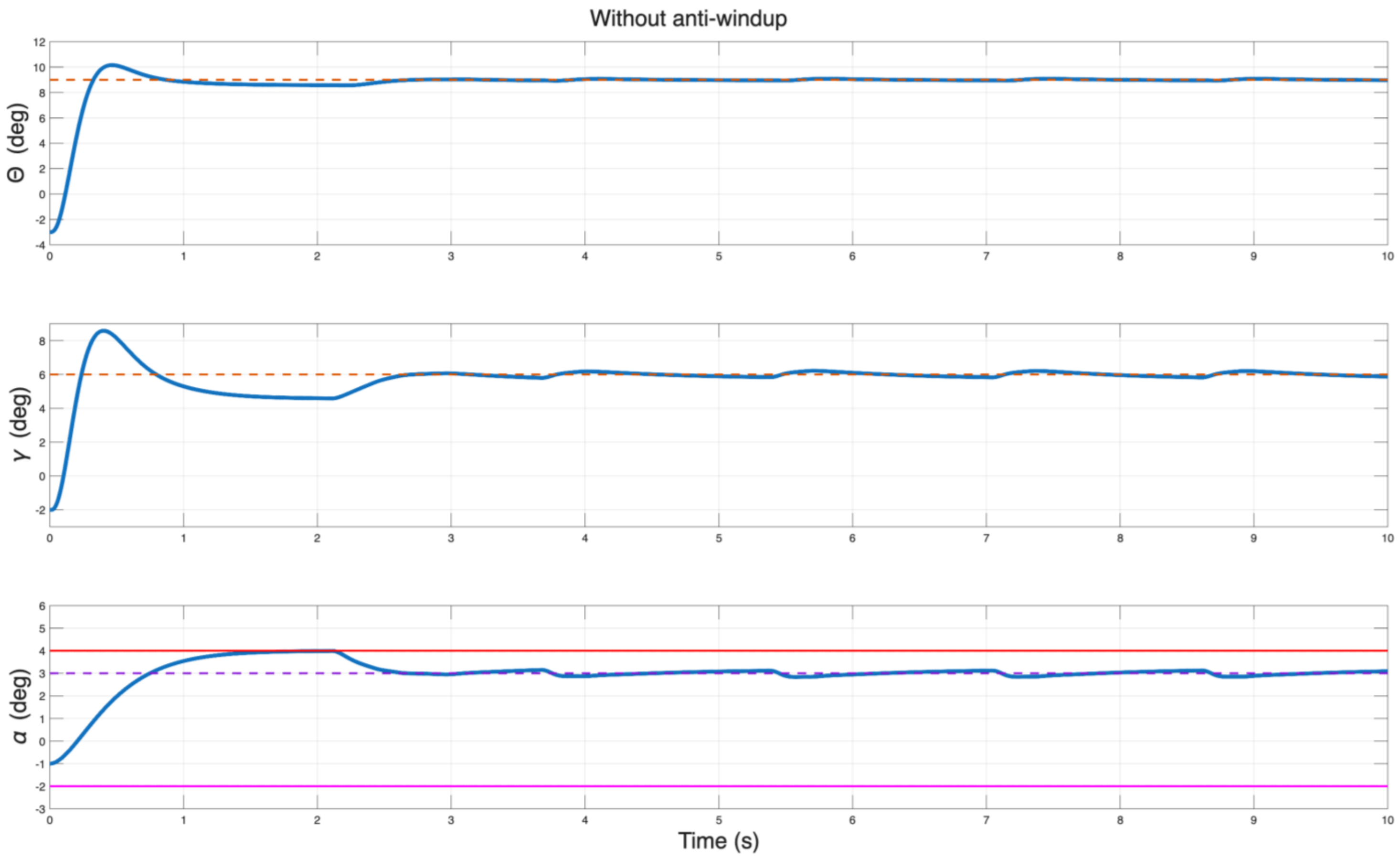

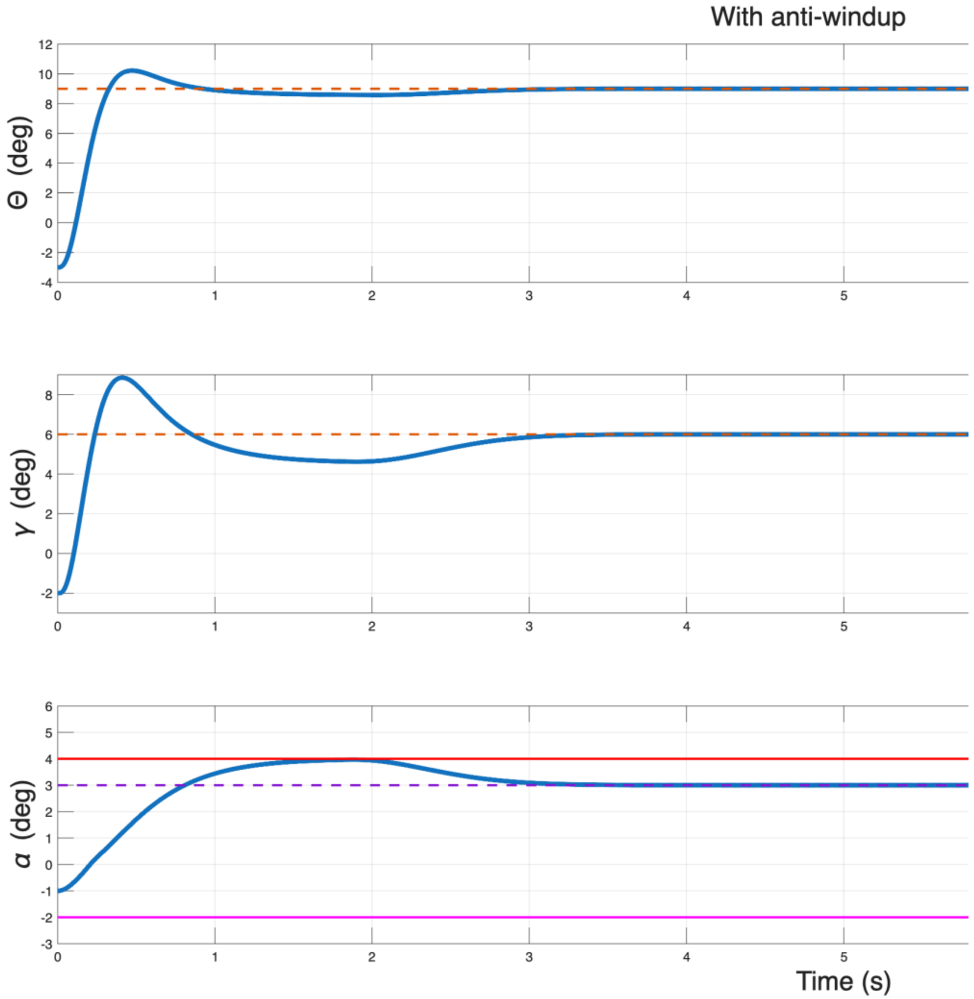

OISTer (extension for robustness)

Class of systems:

$$
\begin{aligned}
\dot{\boldsymbol{x}}(t) &= \mathbf{A}(\boldsymbol{\theta})\,\boldsymbol{x}(t) + \mathbf{B_u}u(t) + \mathbf{B_d}(\boldsymbol{\theta})\,\boldsymbol{d}(t) \\
\boldsymbol{y}(t) &= \mathbf{C}(\boldsymbol{\theta})\,\boldsymbol{x}(t) + \mathbf{D_u}(\boldsymbol{\theta})\,u(t) + \mathbf{D_d}(\boldsymbol{\theta})\,\boldsymbol{d}(t) \\
\alpha(t) &= \mathbf{C}_{\boldsymbol{\alpha}}\boldsymbol{x}(t) \\
\dot{\boldsymbol{x}}_K(t) &= \mathbf{A_K}\boldsymbol{x}_K(t) + \mathbf{B_K}\boldsymbol{y}(t) \\
y_K(t) &= \mathbf{C_K}\boldsymbol{x}_K(t) + \mathbf{D_K}\boldsymbol{y}(t)
\end{aligned}
$$

Constraint:

$$\alpha(t) \in \Omega_\alpha(t) = [\underline{\alpha}(t), \overline{\alpha}(t)]\,,\ \forall t \in \mathbb{R}_+$$

OISTer (extension for robustness)

General case: $z = Cx; z^{(r)} = CA^r x + \underbrace{CA^{r-1}B}_{\neq 0} u$

OIST

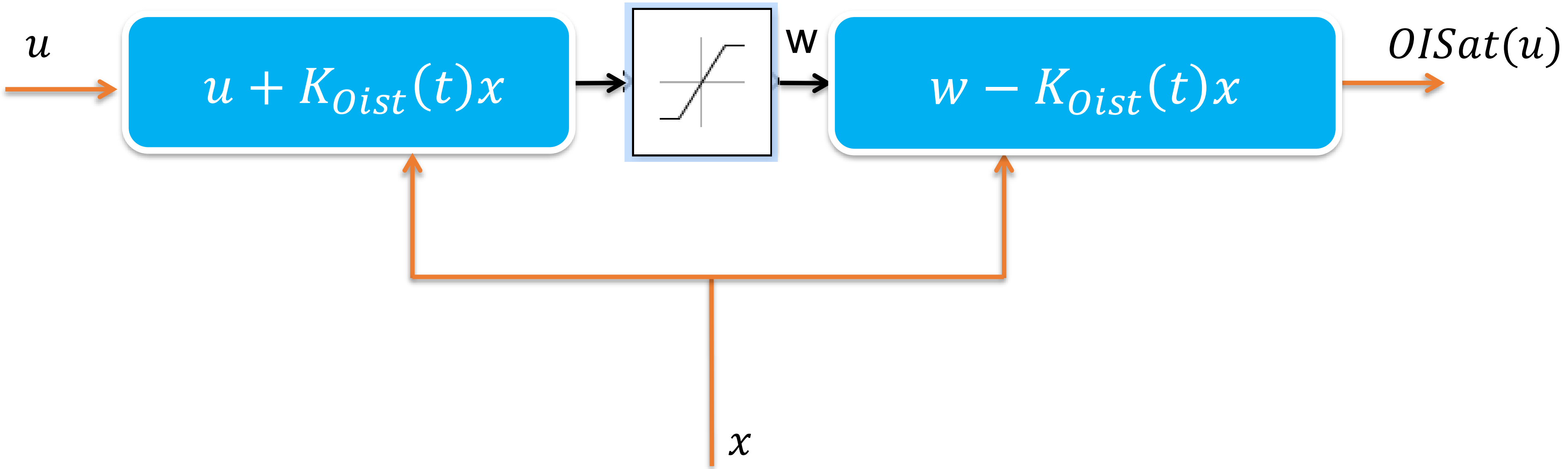

+ 2r inequalities : $L_{Oist}\, x(0) \leq 1$

OISTer (extension for robustness)

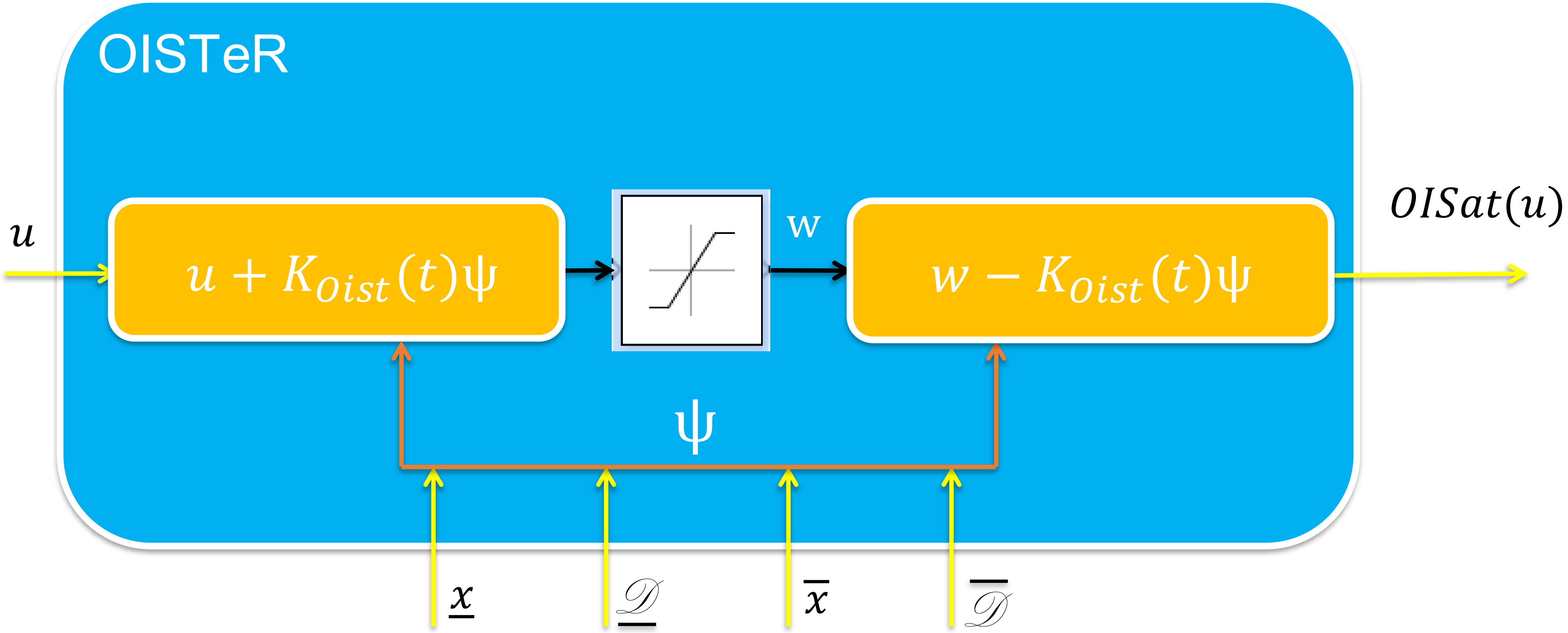

+ 2r inequalities : $L_{Oister}\ x(0) \leq 1$

Burlion Research Group

OISTer (extension for robustness)

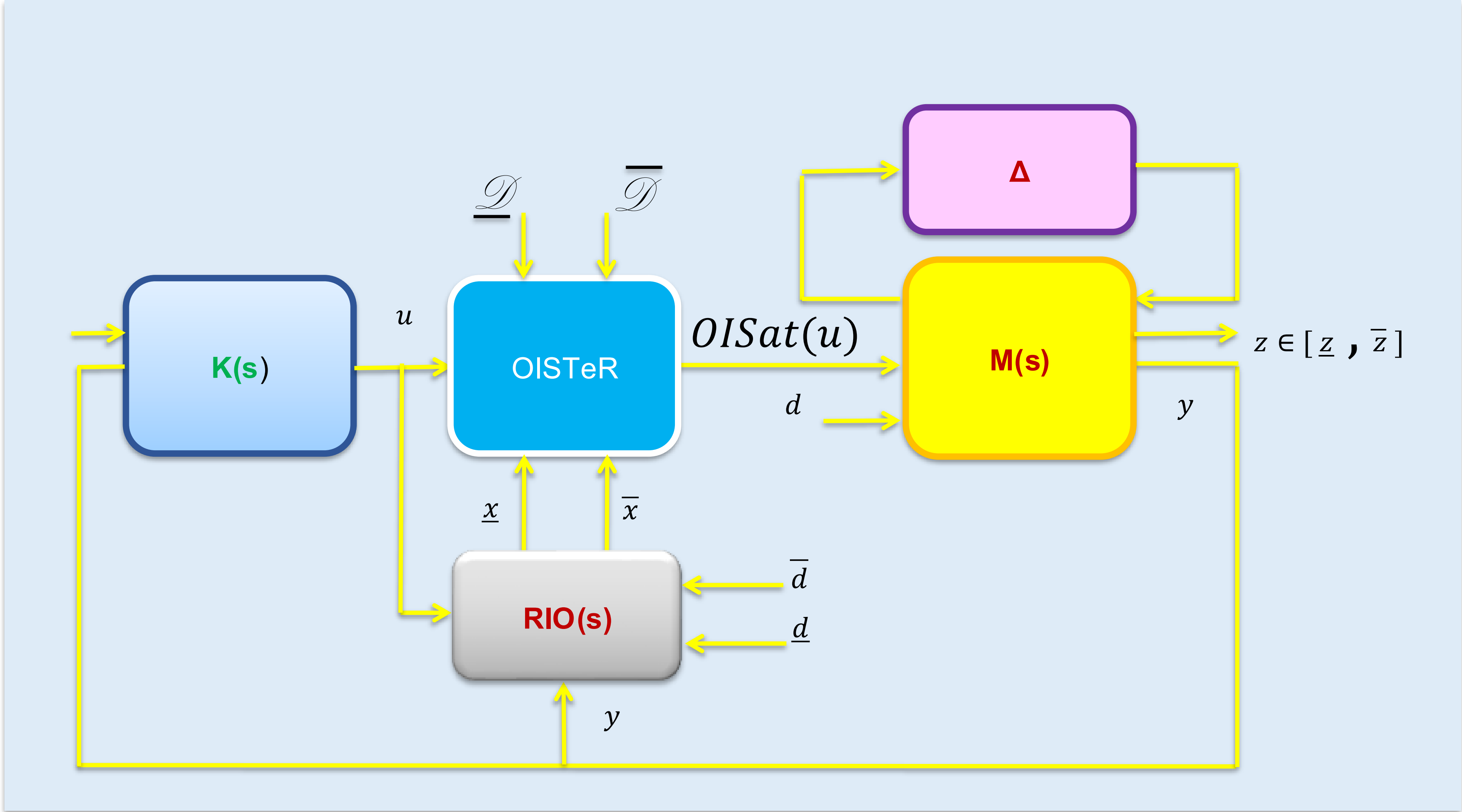

III – Aerospace applications of OISTer

Background
- Motivation
- Output to Input Saturation Transformation (OIST)
- Links between Output to Input Saturation Transformation (OIST) & CBFs

A few technical results
- OIST and bounds overlapping
- Anti-windup designs
- OIST robustness using interval methods (OISTer)

Aerospace applications

Aerospace Applications

ENGINEERING

Collision avoidance of multiple UAVs

UAV obstacle avoidance using a monocular camera

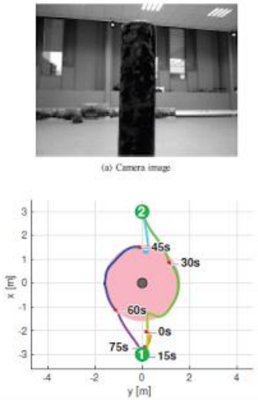

Load control of a flexible large scale airliner model

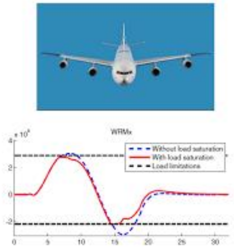

Flexible Launcher GNC with constrained angle of attack

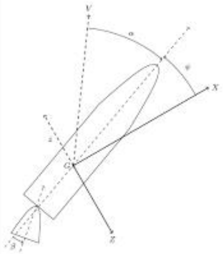

Upset recovery of a UAV

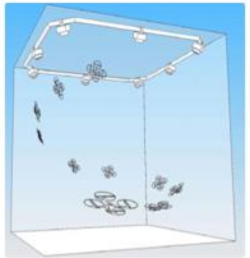

Vision based landing of a UAV

Nonlinear control of a satellite with fuel slosh

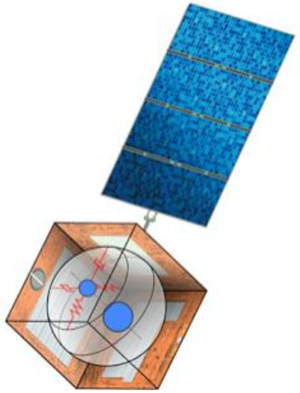

Soft Lunar landing using optic flow sensors

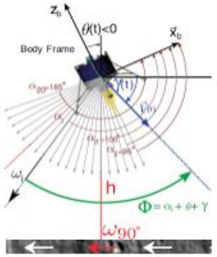

Sponsors:

EUROPEAN DEFENCE AGENCY

Clean Sky

EUROPEAN COMMISSION

esa

cnes CENTRE NATIONAL D'ÉTUDES SPATIALES

AIRBUS DEFENCE & SPACE

Agence Nationale de la Recherche ANR

Burlion Research Group

1- Launcher

From E. Chambon (Ph.D dissertation, 2018).

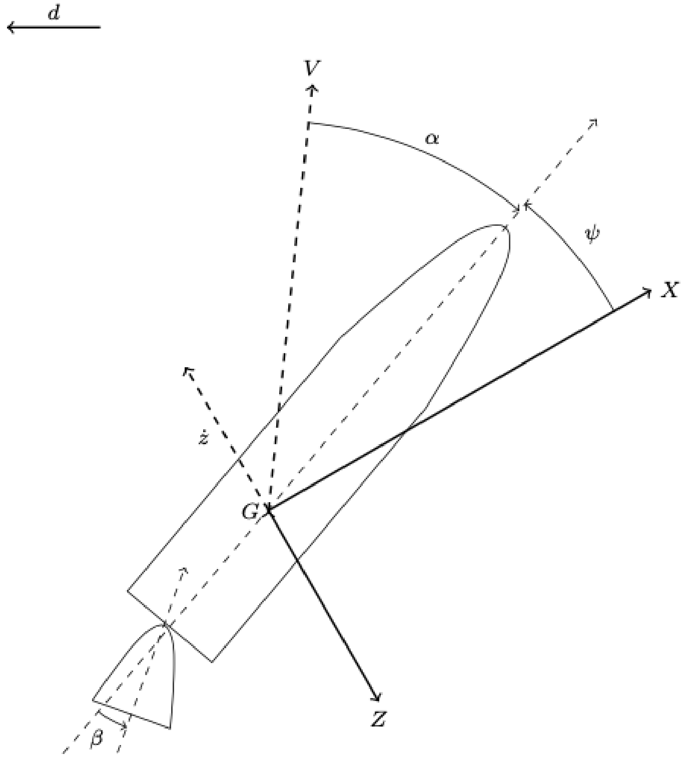

$$(\mathbf{G}) \begin{cases} \dot{\boldsymbol{x}}^1 = \begin{bmatrix} 0 & 1 & 0 \\ A_6 & 0 & \frac{A_6}{V} \\ a_1 & 0 & a_2 \end{bmatrix} \boldsymbol{x}^1 + \begin{bmatrix} 0 & 0 \\ -\frac{A_6}{V} & K_1 \\ -a_2 & a_3 \end{bmatrix} \begin{bmatrix} d \\ \beta \end{bmatrix} \\ \boldsymbol{z} = \begin{bmatrix} 1 & 0 & \frac{1}{V} \\ 0 & 0 & 1 \end{bmatrix} \boldsymbol{x}^1 + \begin{bmatrix} -\frac{1}{V} & 0 \\ 0 & 0 \end{bmatrix} \begin{bmatrix} d \\ \beta \end{bmatrix} \\ \boldsymbol{y} = \begin{bmatrix} 1 & 0 & 0 \\ 0 & 1 & 0 \end{bmatrix} \boldsymbol{x}^1 \end{cases}$$

where $\boldsymbol{y} = \begin{bmatrix} \psi \\ \dot{\psi} \end{bmatrix}$ is the measurements vector and $\boldsymbol{z} = \begin{bmatrix} \alpha \\ \dot{z} \end{bmatrix}$.

Unmeasured constrained output: $\alpha = \psi + \frac{\dot{z} - d}{V}$

ENGINEERING

Technical difficulties

- The constrained output is unmeasured: $\alpha = \psi + \frac{\dot{z} - d}{V}$ → Use interval methods
- It is NMP: $T_{\beta \to \tilde{\alpha}}(s) = \frac{K\left(s+z_1\right)\left(s-z_2\right)}{\left(s-p_1\right)\left(s-p_2\right)\left(s-p_3\right)}$ → Use an approximated output

Burlion Research Group

1- Launcher

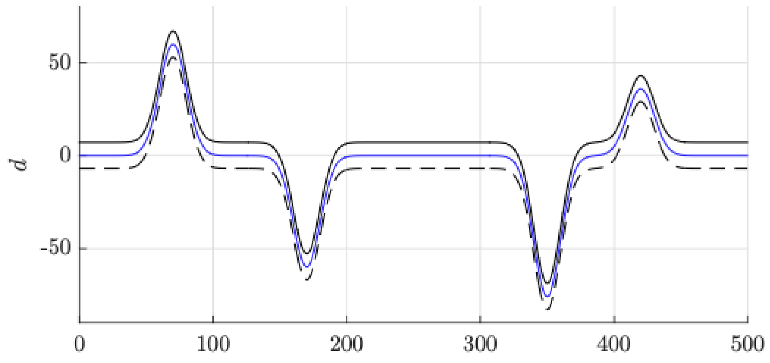

Custom wind profile

Results

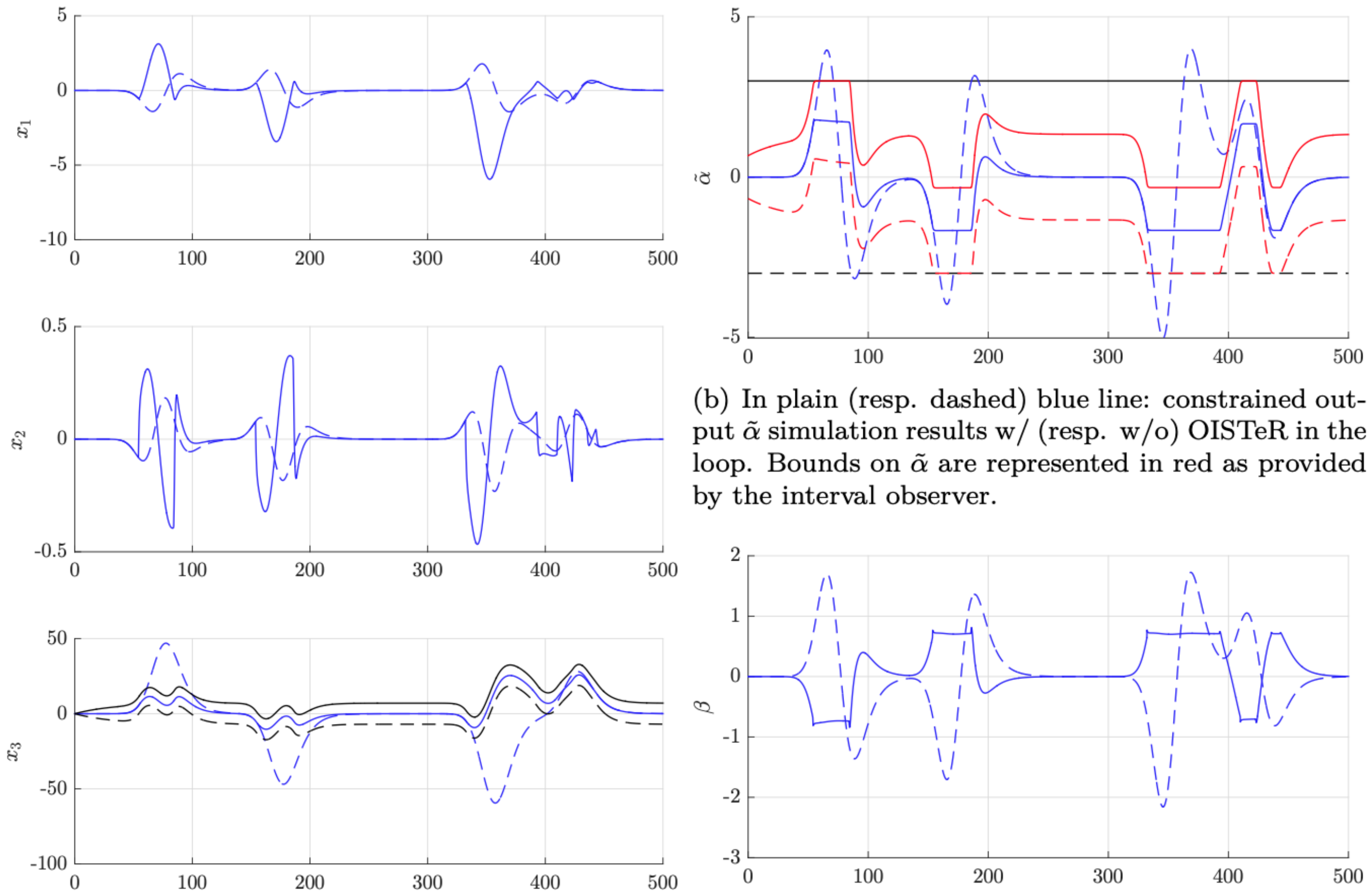

(a) State simulation results w/ (resp. w/o) OISTeR in the loop in plain (resp. dashed) blue. The reduced-order interval observer on $\boldsymbol{x}_3$ output is represented in black lines.

(b) In plain (resp. dashed) blue line: constrained output $\tilde{\alpha}$ simulation results w/ (resp. w/o) OISTeR in the loop. Bounds on $\tilde{\alpha}$ are represented in red as provided by the interval observer.

(c) In plain (resp. dashed) blue line: control input u simulation results w/ (resp. w/o) OISTeR in the loop. In the OISTeR case, the control input is given by $\beta = -\boldsymbol{K}\boldsymbol{x} + v$.

Cleansky JTI project (2011 – 2013)

(From Burlion et al., IFAC WC 2014)

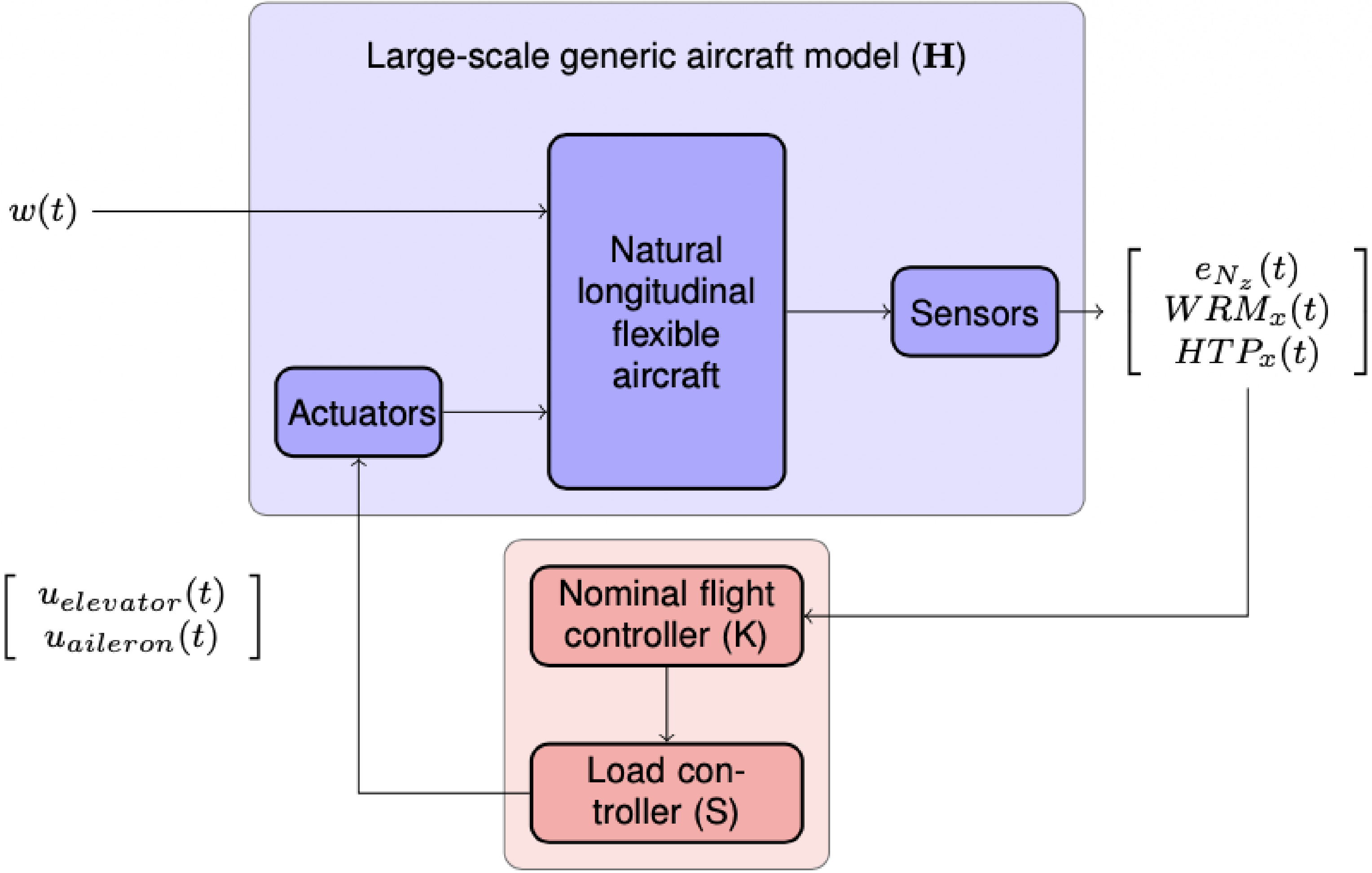

Burlion Research Group

Technical difficulties

- This is a high-dimensional model → Use "OIST"
- The constrained output is NMP → Use an approximated output

Numerical results of a maneuver vertical stretched

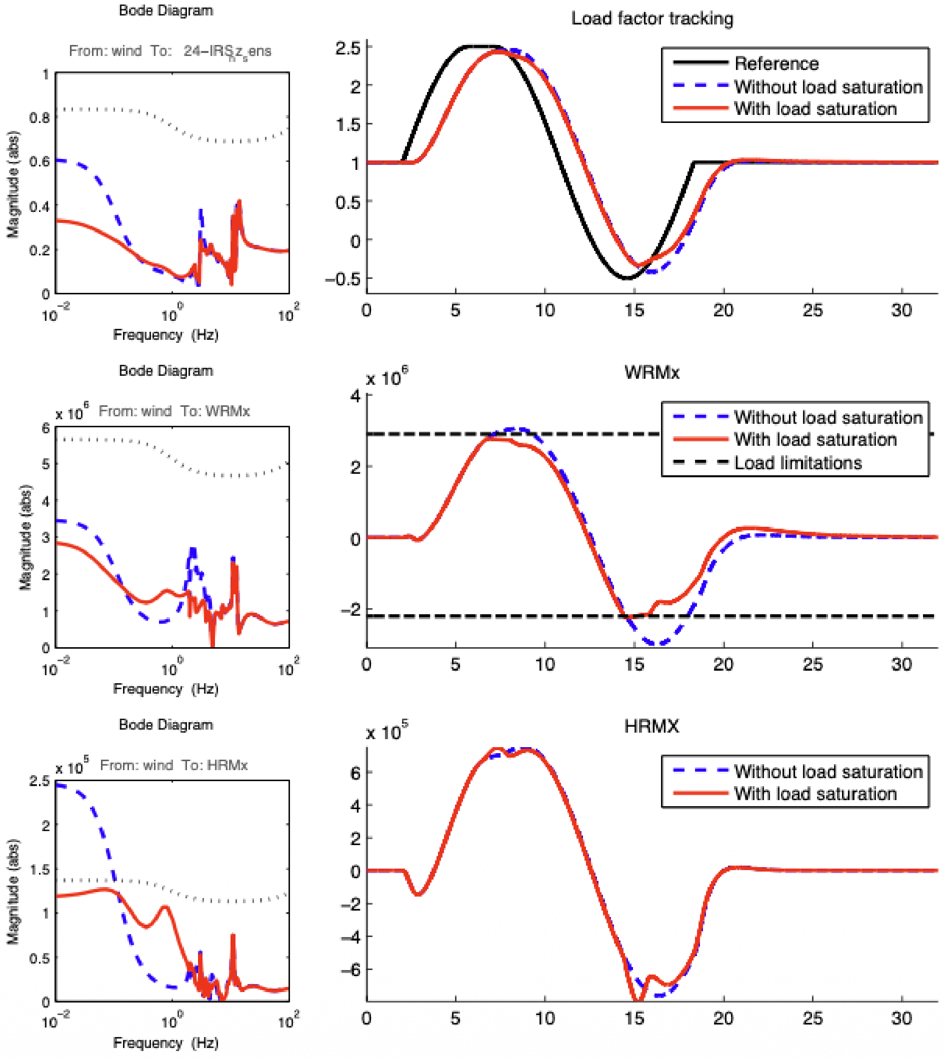

C. Poussot-Vassal & L. Burlion
ONERA DCSD

Closed-loop stable

Gain over [0.1 100]Hz:
$\frac{\mathcal{J}^{nom} - \mathcal{J}}{\mathcal{J}^{nom}}$ =25.4701 %

$\mathcal{H}_\infty$ attenuation: γ =1.6236

Controller with:
* n_c =10 poles (0 unstable)
* n_u =3 input(s)
* n_y =2 output(s)

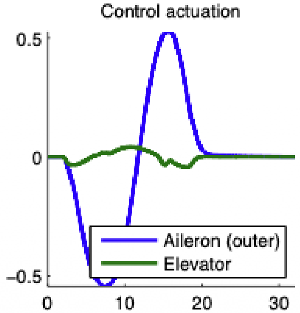

(From Burlion et al., IFAC WC 2014)

3- Satellite attitude tracking

From L. Burlion, J.M Biannic and T. Ahmed-Ali, "*Attitude tracking of a flexible spacecraft under angular velocity constraints*", International Journal of Control, 2018.

$$\dot{q}_e = \frac{1}{2} E(q_e)\omega_e$$

$$J_{mb}\dot{\omega}_e = -N(\omega, \omega_e, z_e, \omega_r^b) + u + d + C_z z_e + D_z \omega_e - J_{mb}\dot{\omega}_r^b$$

$$\dot{z}_e = A_z z_e + B_{1,z}\omega_e + B_{2,z}\dot{\omega}_r^b$$

(Error Model from Di Gennaro 2002)

Burlion Research Group

3- Satellite attitude tracking

Technical difficulties

- Angular velocity constraints
- Nonlinear model (gyroscopic term, quaternion usage)
- Unmeasured torque disturbance
- Unmeasured flexible modes

Solution

Interval observer

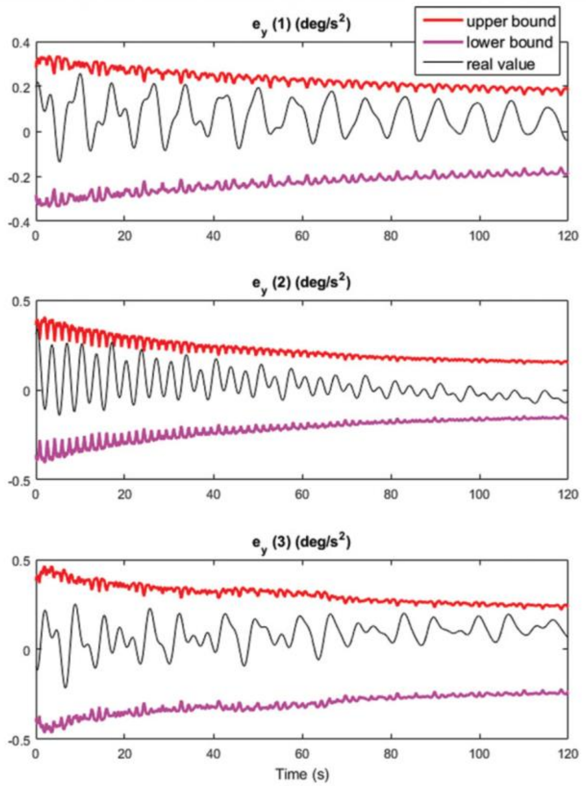

Nonlinear controller+OISTer+Anti-windup

$$u = OISat(\tilde{u}_n + u_a)$$

$$= J_{mb}\left(Sat_{k(t)\underline{\omega}+\bar{e}_y}^{k(t)\overline{\omega}-\bar{e}_y}(\alpha + k(t)\omega) - k(t)\omega\right) + N(\omega, \omega, \hat{z}, 0) - C_z\hat{z} - D_z\omega$$

$$\dot{q}_a = \frac{1}{2}E(q_a)\omega_a := \frac{1}{2}E(q_a)R(q_e)R(q_a)^T\omega_a^{be}$$

$$J_{mb}\dot{\omega}_a^{be} = (N(\tilde{\omega} + \omega_r^b, \tilde{\omega}, \hat{\tilde{z}}, \omega_r^b) - N(\omega, \omega_e, \hat{z}_e, \omega_r^b)) + C_z z_a + D_z\omega_a^{be} + OISat(\tilde{u}_n + u_a) - \tilde{u}_n$$

$$\dot{z}_a = A_z z_a + B_{1,z}\omega_a^{be}$$

3- Satellite attitude tracking

- From L. Burlion, J.M Biannic and T. Ahmed-Ali, "*Attitude tracking of a flexible spacecraft under angular velocity constraints*", International Journal of Control, 2018.

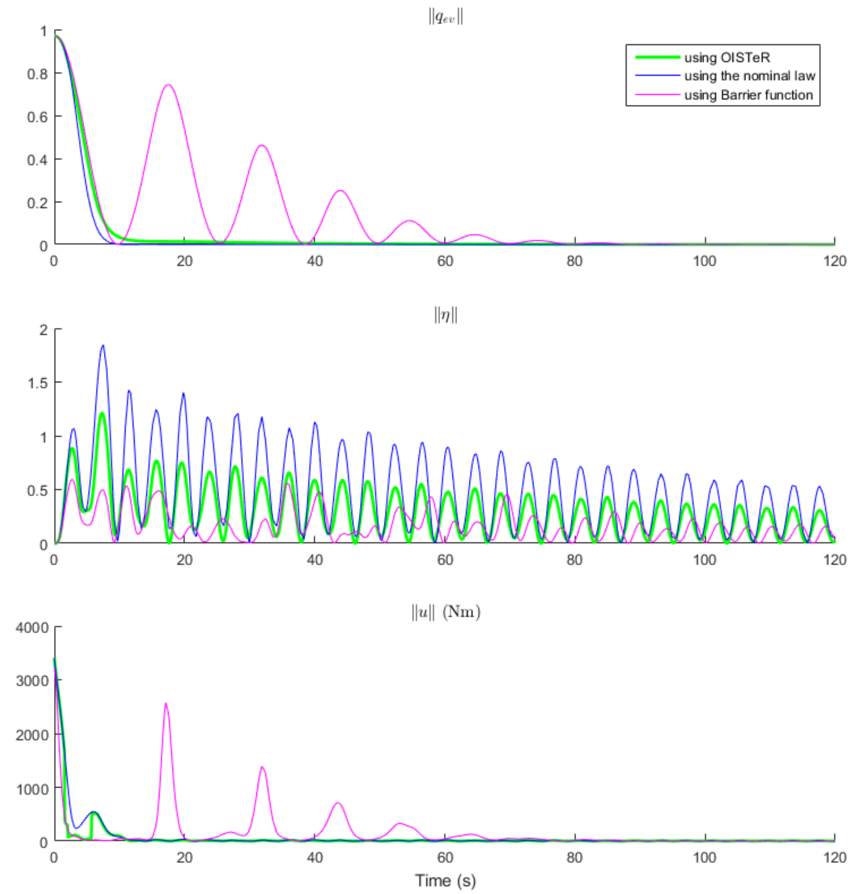

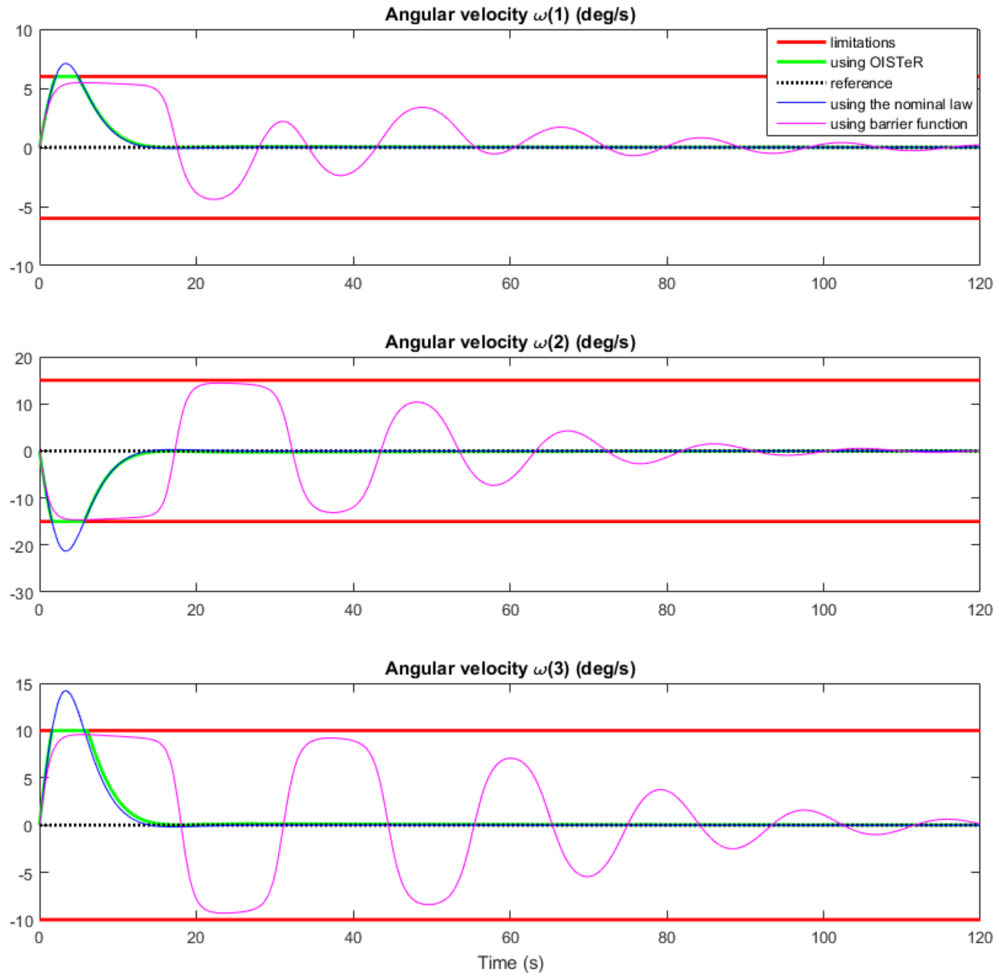

Burlion Research Group

Conclusions

Thank you for your attention!

References

ENGINEERING

- L. Burlion, “A new saturation function to convert an output constraint into an input constraint,” in Proc. of the 20th Mediterranean Conference on Control and Automation, MED, pp. 1217–1222, 2012.
- L. Burlion and H. de Plinval, "Keeping a Ground Point in the Camera Field of View of a Landing UAV", in Proc. of the IEEE International Conference on Robotics and Automation, ICRA, pp. 5763-5768, 2013.
- L. Burlion, C. Poussot-Vassal, P. Vuillemin, M. Leitner, and T. Kier, "Longitudinal Maneuver Load Control of a Flexible Large-Scale Aircraft," in Proc. of the 19th IFAC World Congress, IFAC WC, pp. 3413-3418, 2014.
- E. Chambon, L. Burlion, and P. Apkarian, “*Robust output interval constraint using O/I saturation transformation with application to uncertain linear launch vehicle*,” in Proc. of the European Control Conference, ECC, pp. 1796-1801, 2015.
- C. Chauffaut, F Defaÿ, L Burlion, and H de Plinval, "UAV obstacle avoidance scheme using an Output to Input Saturation Transformation technique," in Proc. of the International Conference on Unmanned Aircraft Systems, ICUAS, pp. 227-234, 2016.
- E. Chambon, L. Burlion and P. Apkarian, “*Time-response shaping using Output to Input Saturation Transformation*,” International Journal of Control, vol. 91(3), pp.534-553, 2018.
- L. Burlion, J.M Biannic and T. Ahmed-Ali, “*Attitude tracking of a flexible spacecraft under angular velocity constraints*,” International Journal of Control, vol. 92(7), pp.1524-1540, 2019.
- L. Burlion, L. Zaccarian, H. de Plinval, and S. Tarbouriech, “Discontinuous model recovery anti-windup for image based visual servoing,” Automatica, vol.104, pp.41-47, 2019.
- C. Zhao, M. Fogel and L. Burlion, "Control of propellant slosh dynamics in observation spacecraft using Model Free Control and pressure sensors,” IEEE Conference on Control Technology and Applications, CCTA, pp. 191-196, 2022.

Burlion Research Group